Computational and Parametric Analysis of Parabolic Trough Collector with Different Heat Transfer Fluids

Rupinder Singh(✉), Yogender Pal Chandra, and Sandeep Kumar

Mechanical Engineering Department, Thapar University,
Patiala 147004, Punjab, India
rupinderratan4@gmail.com

Abstract. Solar energy is abundantly available on earth. The temperature of heat source needs to be high for the higher efficiency; be it energy production through thermodynamic cycle or heat extraction using heat transfer media, and solar energy concentration devices helps in achieving high temperature. Parabolic trough collector (PTC) has its own advantage with concentration ratio upto 215 times with reasonable cost and operational convenience, especially when low to medium range temperature heating is required. Present work is focused on the experimental and computational study on PTC with different heat transfer fluids towards identifying a suitable heat transfer fluid and flow parameters towards achieving higher heat collection and transfer efficiency. Most decisive thermo-physical entity such as heat transfer fluid (HTF) and its property *i.e.* flow rate is varied and its influence on the thermal efficiency, heat transfer and net effective temperature gain is analysed with the numerical model and results validated with experimental work. For numerical study, computational fluid dynamics (CFD) approach is taken using ANSYS–fluent software package. The experimentation results are in good agreement with the numerical model and suggest that with the flow rates of different HTF maintained within 3–5 LPM, the temperature gain can be achieved between 3–6 °C in a single pass with a maximum efficiency of 59.7%.

Nomenclature

CFD	Computational Fluid Dynamics
CSP	Concentrated Solar Power
HTF	Heat Transfer Fluid
PTC	Parabolic Trough Collector
TES	Thermal Energy Storage
Re	Reynolds Number
ρ	Density
u	Velocity in x-direction
δ_{ij}	Intermolecular Distance
T	Temperature
g_i	Gravitational Acceleration
λ, C_P	Constant
S_T	Momentum Source

K. Deep et al. (eds.), *Proceedings of Sixth International Conference on Soft Computing for Problem Solving*, Advances in Intelligent Systems and Computing 547,
DOI 10.1007/978-981-10-3325-4_32

1 Introduction

Concentrated solar power (CSP) has been a subject of great interest worldwide for several decades with Spain in its leading rein [1]. Concentrating solar energy employs a complicated scheme of mirrors or mirror finished curved metallic plates with a sun tracking arrangement, heat transfer fluids to transport the necessary thermal energy to the power block where it can be fed to power turbine to generate electricity using thermodynamic cycle, or can be used for thermal application.

Parabolic trough collector (PTC) is a mature solar thermal technology and is used widely for various industrial heating application and is very useful while working below 400 °C [2]. PTC comprises of a mirror finish curved metallic plate bent into parabolic shape so as to linearly focus all the incident radiation onto the absorber tube. In some large application, many of such sheets are put together to form a long arrays of troughs. The receiver/absorber system which is typically a metal pipe enclosed in an evacuated glass tube to reduce the convection losses, is mounted on the focus of the collector. To increase the thermal effectiveness and minimize the losses, anti-reflective coating is also applied on metal pipe.

Concentration ratio is defined as ratio of the collector's aperture area to the receiver area [3]. Characteristically, concentrating collectors can own different concentration ratio henceforth can operate at different temperatures. It should be noted that efficiency of the heat transfer or power production through thermodynamic cycle is a direct function of the operating temperature. However, practically, material of concentrating system, heat transfer fluid, storage system and the type of power cycle are sole decisive factors [4].

Primarily, the function of the collector is to focus the incident solar radiations onto the receiver/absorber system which is a heat exchanger device from where heat is carried away by heat transfer fluid (HTF). Heat transfer fluid is one of the critical constituent for the overall performance of the CSP. HTF can also be used as thermal energy storage (TES) device, storing heat in insulated TES tanks. Most suitable characteristics of the HTF includes thermal stability, high boiling point, high thermal conductivity, low melting point, high specific heat capacity for energy storage purpose and low viscosity [5]. Depending on the working temperature and end use, suitable HTF is used. HTF's could be assorted into six groups namely air or other gases; water/steam; Thermal oil; organics; molten-salts; liquid metals. Different researchers has used different types of materials for heat absorbing tube, such as copper, stainless steel, brass, etc. along with different type of absorbing fluid materials such as, Nano fluid, thermal oil, molten salt, water, air, etc. [6–8].

Air can be used for a wide range of temperatures and can be heated up to 700 °C at atmospheric pressure [5] and further can be used for steam generation while exchanging its heat with water in heat exchanger. Low specific heat, thermal conductivity and density of air result in low thermal density which makes it comparatively uncommon HTF choice in large size solar thermal plants. Water both as HTF and working fluid (called direct steam generation, DSG), complications are simplified many folds and the result is improved cycle efficiency and decreased power cost [9]. Most primary of thermal oils includes synthetic oils, silicone oils and mineral oils. Thermal stabilities of these oils break at around 400 °C and that's the reason they are

used for low temperature applications [6]. On the other hand, organics like Biphenyl/Diphenyl oxide or TherminolVp-1™ in common jargon is a big success in commercial CSP plants. TherminolVp-1, a universally accepted organic oil, is a eutectic agglomeration of two very stable compounds Biphenyl ($C_{12}H_{10}$) and Diphenyl Oxide ($C_{12}H_{10}O$) [5] and has very favorable working range for practically any PTC operations such as industrial process heat and power generation. Furthermore, a molten salt makes an excellent HTF's due to most favorable thermal stability at elevated temperatures (above 1000 °C). Molten salts are most pioneering technology used by state of the arts CSP plants based in France, United States and Spain. Most of its typical salts are based on nitrates or nitrites such as $NaNO_3$ (60 wt. %) & KNO_3 (40 wt. %). Liquid metals have not been used yet in CSP technology, though; they show very good thermo physical characteristics which makes them suitable for a HTF.

The present paper uses conventional water based and oil based HTF's such as water, endethylene glycol, ThermnolVp-1™ and Mythol-Therm 500. Secondly, experimental work is followed with theoretical modeling of receiver tube for various mass flow rates of HTFs with the use of CFD based ANSYS- Fluent software. To further illustrate, mass flow rate of each fluid was varied in range of 0.043–0.091 kg/s.

2 Experimental Setup

The experimental setup is a single axis tracking, 1.22 m long and single trough test rig situated at Thapar University, Patiala, Punjab. The major components of test facility includes stainless steel collector with mirror finish curved metallic sheet having arch

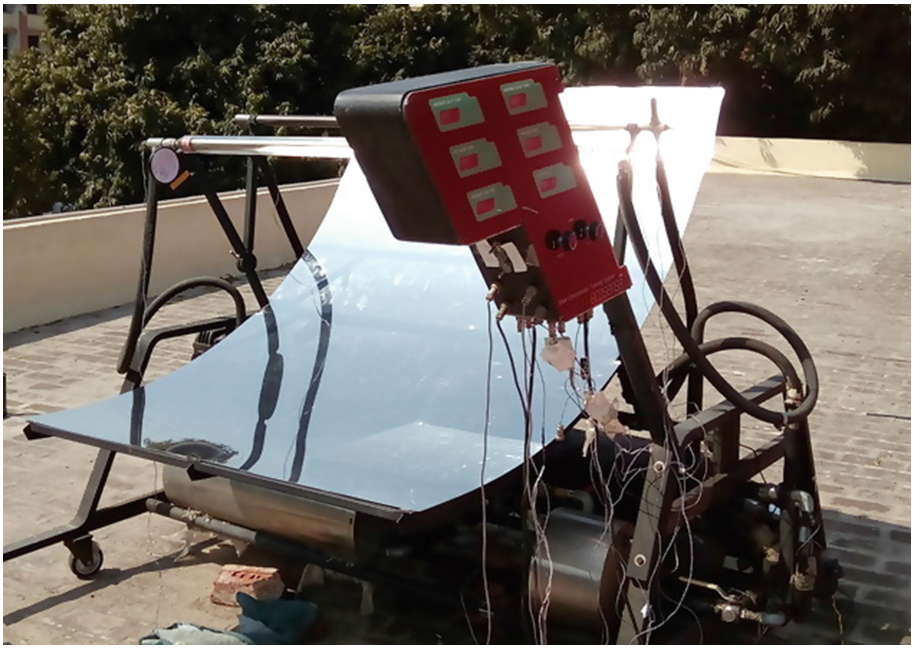

Fig. 1. Experimental test rig (TU)

Table 1. System specification.

Total aperture area of solar field	8175 m^2
Length of PTC	121.9 cm
Focal length	60.7 cm
Aperture width	197 cm
Outer diameter of absorber	3.1 cm
Inner diameter of absorber	2.8 cm
Outer diameter of glass envelop	4.5 cm
Inner diameter of glass envelop	3.9 cm
Absorber tube material	Copper
Absorber glass material	Silicate glass
Rim angle	81°
Concentration ratio	50

length 1.83 m and focal length of 0.613 m, copper absorber tube with absorptance of 0.89, diameter of 0.03 m and length 1.2 m. Absorber tube is air filled annulus with glass envelope having transmittance of 0.95 and emittance of about 0.84. An east to west tracking system powered by stepper motors is also tuned up with the PTC to effectively track the sun movement for enhanced solar energy collection. A 28 L stainless steel storage tank is incorporated with the system with glass wool insulation. Figure 1 depicts the schematic of test rig while, Table 1 demonstrates its specification.

3 Numerical Method

For experimental validation, computational fluid dynamics (CFD) is used which entails the geometric modeling of receiver in ANSYS geometric modeler. After successful modeling, the model is imported for meshing and specific named selection is performed to differentiate each part of receiver such as glass envelop, air annulus, and inlet and outlet. Energy conservation equation is used in ANSYS-Fluent to solve the heat conduction and heat transfer problem. To simulate the turbulent flow condition, k-ε model is turned on. Radiation heat exchange on receiver is simulated by invoking solar S2S model. Furthermore, for comparison of thermal efficiency of receiver, 4 types of working fluids were used which are categorized under conventional and high grade industrial acquainted water based and oil based HTFs. Table 2 describes the material and their thermo-physical properties assigned in material section of Fluent.

3.1 Governing Equations

For fluid flow, Navier-Stokes equation is invoked which takes into account for continuity, energy and momentum equations. Furthermore, to define heat transfer in fluid, energy conservation equation which includes convection in fluid and conduction in absorber tube is invoked in the solution procedure. For radiation heat exchange,

Table 2. Thermo physical properties of material used

Material	K (W/m-k)	ρ (kg/m^3)	C_p (J/kg-k)	μ (kg/m-s)
Air	0.0242	1.125	1006.43	0.00001789
Water	0.622	1000	4180	0.001003
Mythol-Therm500	0.102	868	2150	0.002430
Ethylene Glycol	0.254	1110	2430	0.001587
TherminolVp-1	0.117	1068	2270	0.004570
Copper	387.6	8978	381	–

radiation model is invoked. Employing turbulent flow RNG k-ε model for which turbulent intensity is calculated by the flowing relation [10].

$$k_{in} = 0.16(\mathrm{Re}_{Dh})^{-\frac{1}{8}} \times 100\% \tag{1}$$

Following are the principle equations solved for current problem by numerical approach of CFD

Continuity equation:

$$\frac{\partial \rho}{\partial t} + \frac{\partial}{\partial x_i}(\rho u_j) = 0 \tag{2}$$

Momentum equation:

$$\frac{\partial}{\partial t}(\rho u_i) + \frac{\partial}{\partial x_i}(\rho u_i u_j) = \frac{\partial}{\partial x_j}\left[-\rho\delta_{ij} + \mu\left(\frac{\partial u_i}{\partial x_j} + \frac{\partial u_j}{\partial x_i}\right)\right] + \rho g_i \tag{3}$$

Energy equation:

$$\frac{\partial}{\partial t}(\rho c_p T) + \frac{\partial}{\partial x_i}(\rho u_i c_p T) - \frac{\partial}{\partial x_j}\left(\lambda \frac{\partial T}{\partial x_j}\right) = s_T \tag{4}$$

3.2 Geometry and Grid Generation

After properly designing the receiver tube in design modeler of ANSYS, it is exported for mesh generation where its domain is discretized into finitude of smaller sub-elements. Figure 2(a), (b) and (c) describe the modelled geometry, isometric and front view respectively of grid generated in the modelled receiver.

3.3 Boundary Conditions

Boundary conditions are needed to be identified which includes no slip condition for fluid flow over wall; Pressure outlet conditions accounting for fully grown viscous flow

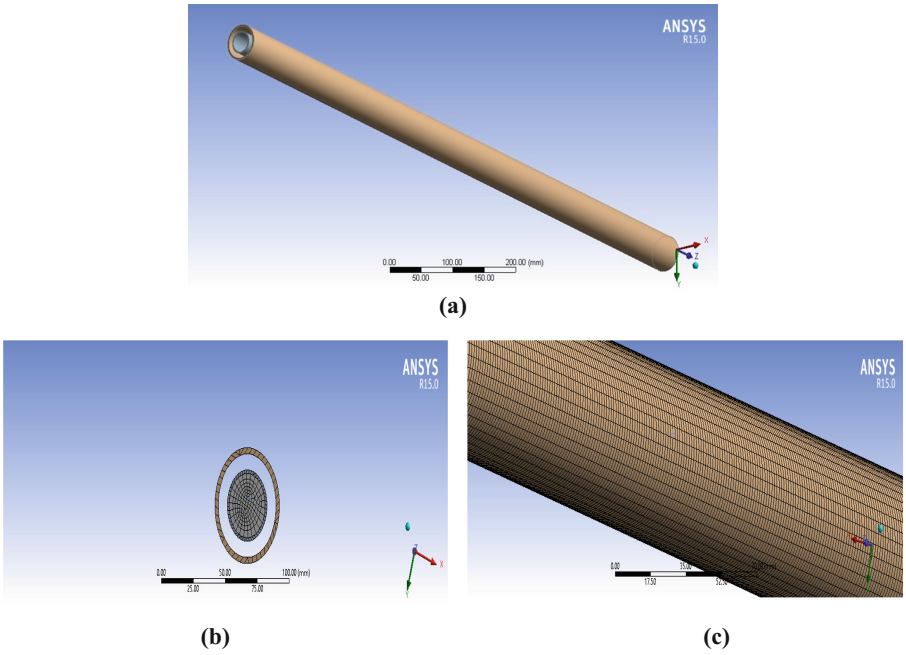

Fig. 2. (a) Physical model of receiver, grid generation in (b) isometric view of receiver, and (c) front view of receiver.

of dissimilar and viscid HTF used in experimentation; non zero heat flux condition at outer surface of absorber tube; constant heat flux around the absorber. Finally, radiation model is invoked and internal emissivity of receiver tube and glass material is set to 0.32 and 0.84 respectively. Appropriate cell zone conditions are given to emulate the receiver well closely to various documented cases in literature [11].

4 Results and Discussions

Experiment was performed for two velocities of HTF *i.e.* 0.066 m/s and 0.11 m/s (3 and 5 LPM respectively). As explained above, variant of fluids were used to compare the existing state of affairs to the new state of the art fluids so as to explain the increase in efficiency in setup. Firstly, conventional fluids *i.e.* water and Mythol–Therm 500 are experimented for the two described velocity and afterwards, high end fluids *viz.* Ethylene glycol and TherminolVp-1 is tested upon for the same parameters.

4.1 Water Based Heat Transfer Fluids

Figure 3 demonstrates the efficaciousness of the conventional receiver in terms of thermal efficiency and outlet temperature for different velocities of fluid flow. To illustrate, water leads to lowest thermal efficiency at flow rate of 0.11 m/s *i.e.* 46.7%, while it increases to 52.7% at 0.066 m/s. However, the increase in thermal efficiency in case of Ethylene Glycol is comparatively less *i.e.* 43.9% with fluid velocity of 0.066 m/s and 45.2% with fluid velocity of .011 m/s. Furthermore, maximum temperature rise was in a single pass was observed in Ethylene Glycol *i.e.* 4.64 K with the flow velocity 0.066 m/s, and 2.92 K with flow velocity 0.11 m/s. With water, maximum temperature rise was 2.89 K with flow velocity of 0.066 m/s and 1.39 K with 0.11 m/s.

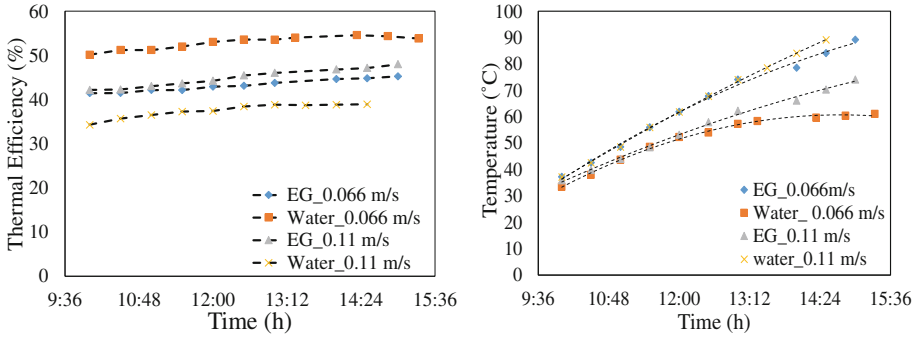

Fig. 3. Influence of mass flow rate of water based HTFs on (a) Thermal efficiency, and (b) Outlet temperature.

In addition, Fig. 4 presents the temperature profile of receivers on both water and Ethylene Glycol. This simulation was carried out for the same fluid velocity as in experimentation. Simulation results are compared with the experimental results and presented in Tables 3 and 5. Thermal efficiency with water having flow velocity 0.11 and 0.066 m/s is evaluated as 55.9% and 50.2% respectively. The mean error between experimental and modeling result is about 6%. While this error is only 2.5% for Ethylene Glycol (refer Tables 3 and 5).

4.2 Oil Based Heat Transfer Fluids

Same operational procedure was adopted for oil based fluids such as Mythol–Therm 500 and TherminolVp-1. Figure 5 presents the result of simulation. It can be inferred from the graphs that TherminolVp-1 has highest thermal efficiency i.e. 56.1% with fluid velocity of 0.066 m/s and 53.4% with fluid velocity of 0.11 m/s. While its 33% with fluid velocity of 0.066 m/s and 32.2% with fluid velocity of 0.11 m/s for Mythol–Therm 500. Furthermore, Mythol–Therm 500 doesn't show such an appreciable change in thermal efficiency with fluid flow velocity though the net temperature rise was far

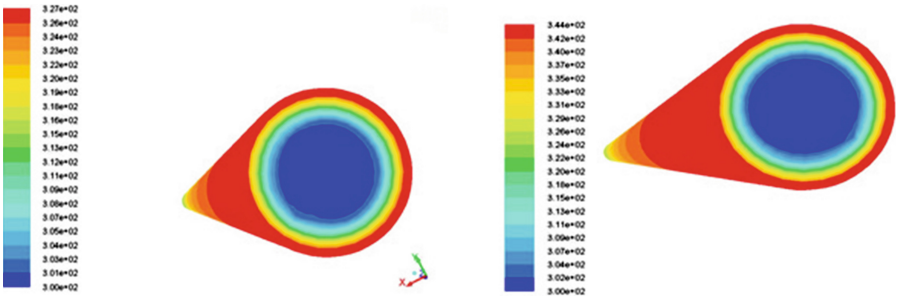

(a) (b)

Fig. 4. Isothermal zones of receiver for HTFs (a) water, and (b) Ethylene Glycol.

Table 3. CFD analyses of both water based HTFs with two different fluid velocities

Flow velocity	0.066 m/s			0.11 m/s		
Fluids	ΔT (K)	Absorber tube temperature (K)	Thermal efficiency (%)	ΔT (K)	Absorber tube temperature (K)	Thermal efficiency (%)
Water	3.4	320.7	55.9	1.89	317.6	50.2
Ethylene Glycol	4.9	334.8	46.4	3.02	330.4	46.5

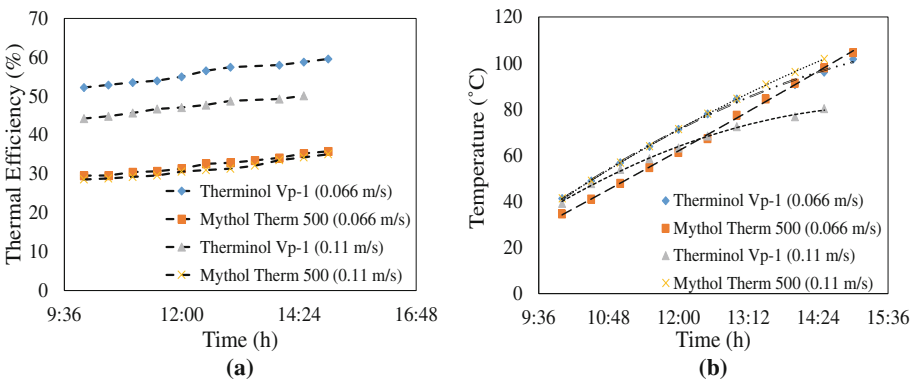

Fig. 5. Influence of mass flow rate of oil based HTFs on (a) thermal efficiency, and (b) outlet temperature.

better than both water, Ethylene Glycol and TherminolVp-1. This fact is further corroborated by Fig. 5(b). Figure 6 explains the isothermal zones of receiver for both HTFs, and its results are presented in Table 4.

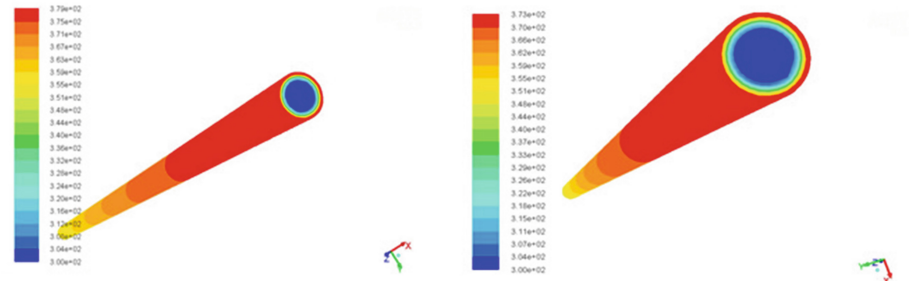

(a) (b)

Fig. 6. Isothermal zones for oil based HTFs (a) TherminolVp-1, and (b) Mythol–Therm 500

Table 4. CFD analyses of both oil based HTFs with two different fluid velocities

Flow velocity	0.066 m/s			0.11 m/s		
Fluids	ΔT K)	Absorber tube temperature (K)	Thermal efficiency (%)	ΔT (K)	Absorber tube temperature (K)	Thermal efficiency (%)
Mythol Therm 500	5.8	362.2	34.2	3.4	356.1	32.9
Therminol Vp-1	6.6	367.8	59.7	4.1	376.4	56.6

Table 5. Comparative stance of modeling and experimentation results

Flow velocity (m/s)	Fluids	CFD Model		Experimental		% Error
		ΔT (K)	Thermal efficiency (%)	ΔT (K)	Thermal efficiency (%)	
0.066	Water	3.4	55.9	2.89	52.7	6.7
	Ethylene Glycol	4.9	46.4	4.64	43.9	2.5
	Therminol Vp-1	6.6	59.7	5.83	56.1	6
	Mythol Therm 500	5.8	34.2	5.61	33.0	3.5
0.11	Water	1.9	50.2	1.39	46.7	6.9
	Ethylene Glycol	3.0	46.5	2.92	45.2	2.7
	Therminol Vp-1	4.2	56.6	3.59	53.4	5.6
	Mythol Therm 500	3.4	32.9	3.32	32.2	2.1

Table 5 demonstrates the comparison between experimental results and the results obtained through computational model of the receiver tube. Result shows a fairly perfect agreement in the experimentation. The distinctive feature of this stance includes the maximum temperature rise in heat transfer fluid in a single pass of receiver and the maximum approachable efficiency of PTC pertaining to that fluid. Maximum temperature rise as well as thermal efficiency of PTC was achieved with therminolVp-1 which is oil based industrial HTF. Secondly, Ethylene Glycol has a moderate efficiency and reasonably good temperature rise. Furthermore, Mythol–Therm 500 also has second most significant temperature gain among the rest of the HTFs (refer Table 5). Water has been evaluated as second most favorable thermal efficiency of PTC. However, thermal efficiency of PTC pertaining to utilization of it is ungainly low.

5 Conclusion

Two groups of HTF were used for the current experimental setup namely conventional and non-conventional water based and oil based fluids respectively. Conventional category includes water as water based and Mythol–Therm 500 as oil based fluid. While, non-conventional fluids are more pushed towards leading industrial usage and includes, Ethylene Glycol as water based and TherminolVp-1 as oil based fluids. Experiments were performed for HTFs at different set of mass flow rate to calculate mean outlet temperature and thermal efficiency of PTC. In addition, computation fluid dynamics approach was adopted to numerically emulate the model and hence to convey numerical validity of the experimentation. Computational model entails proper and realistic geometric and boundary conditions and hence its approaches and checks for veracity of experimentation results. Results showed that TherminolVp-1 is a vanguard of oil based HTF for current setup and increases both thermal efficiency of PTC and outlet temperature of fluid. However, as far as water based fluid is concerned, water has favorable thermo-physical properties if it is used for low temperature applications due to its boiling constraints.

References

1. Antonelli, M., Baccioli, A., Francesconi, M., Desideri, U., Martorano, L.: Electrical production of a small size Concentrated Solar Power plant with compound parabolic collectors. Renewable Energy **83**, 1110–1118 (2015)
2. Zhang, H.L., Baeyens, J., Degreve, J., Caceres, G.: Concentrated solar power plants: review and design methodology. Renew. Sustain. Energy Rev. **22**, 466–481 (2013)
3. Duffie, J.A., Beckman, W.A.: Solar engineering of thermal process. Gear Team (2013)
4. Segal, A., Epstein, M.: Optimized working temperatures of a solar central receiver. Sol. Energy **75**, 503–510 (2003)
5. Tian, Y., Zhao, C.Y.: A review of solar collectors and thermal energy storage in solar thermal application. Appl. Energy **104**, 538–553 (2013)
6. Modi, A., Haglind, F.: Performance analysis of a Kalina cycle for a central receiver solar thermal power plant with direct steam generation. Appl. Therm. Eng. **65**, 201–208 (2014)

7. Beretta, D., Loveless, F.C., Nudenberg, W.: Use of synthetic hydrocarbon oils as heat transfer fluids. US Patent 4239638 (1980)
8. Goods, S., Bradshaw, R.: Corrosion of stainless steels and carbon steel by molten mixtures of commercial nitrate salts. J. Mater. Eng. Perform. **13**, 78–87 (2004)
9. Feldhoff, J.F., Benitez, D., Eck, M., Riffelmann, K.: Economic potential of solar thermal power plants with direct steam generation compared with HTF plants. Sol. Energy **132**, 41–100 (2010)
10. Wilcox, D.C.: Turbulence modelling for CFD. DCW Industries Inc. (1998)
11. Dudley, V., Kolb, G., Sloan, M.: Test results: SEGS LS2 solar collector. Report of Sandia National Laboratories, Sandia 94-1884 (1994)